Two-photon double ionization of H_2 at 30 eV using Exterior Complex Scaling

F. Morales[1] and F. Martín[1]

[1]Departamento de Química C-9, Universidad Autónoma de Madrid, 28049 Madrid, Spain

D. A. Horner[2], T. N. Rescigno[3] and C. W. McCurdy[3,4]

[2]Los Alamos National Laboratory, Theoretical Division, Los Alamos, NM 87545
[3]Lawrence Berkeley National Laboratory, Chemical Sciences, Berkeley, CA 94720
[4]Departments of Applied Science and Chemistry, University of California, Davis, CA 95616

E-mail: `felipe.morales@uam.es`

Abstract. Calculations of fully differential cross sections for two-photon double ionization of the hydrogen molecule with photons of 30 eV are reported. The results have been obtained by using the method of exterior complex scaling, which allows one to construct essentially exact wave functions that describe the double continuum on a large, but finite, volume. The calculated cross sections are compared with those previously obtained by Colgan et al [1], and discrepancies are found for specific molecular orientations and electron ejection directions.

1. Introduction

Double ionization of the helium atom by two XUV photons has recently become the subject of intense theoretical interest (see, e.g. [2, 3, 4, 5, 6, 7, 8, 9, 10, 11, 12, 13, 14, 15, 16, 17, 18, 19]). This interest was first spurred by measurements with high harmonic generation sources in Japan [20] and, more recently, by experiments at the free-electron laser source (FLASH) in Hamburg [21, 22]. A general conclusion of these studies is that, in contrast to single-photon double ionization of Helium, the electrons have a preference to escape back to back, which can be easily recognized in the calculated triply differential cross sections [14, 15, 16] and/or in the measured and calculated recoil ion angular distributions [23]. This conclusion may seem at first surprising since, at variance with the single-photon case, one does not have to invoke electron correlation to induce ejection of both electrons (roughly speaking, a photon is available for each electron and the electrons do not need to talk to each other in order to leave the atom), but so far there is no measurement or recent calculation in contradiction with this finding. There is, however, a question that has led to intense debate in the last few years [7, 8, 9, 10, 11, 12, 13, 14, 15, 16, 17, 18, 19]. This is the absolute value of the two-photon double ionization cross section. In spite of the fact that all these experiments have been performed in the intensity regime where second order perturbation theory is expected to be valid and, therefore, theory is easiest to apply, recent calculated cross sections differ by more than an order of magnitude [15]. Unfortunately, the existing experiments [20, 21, 22, 24] cannot help very much in this debate, since the two-photon double ionization cross section is very small and detection statistics is rather poor. The reasons for such a strong disagreement are still far from being understood.

More recently, experiments under way at FLASH [25] have aimed at studying two-photon double ionization of homonuclear diatomic molecules, in particular H_2. Although H_2 is more complicated than Helium and, consequently, similar discrepancies in the absolute value of the cross section may be expected, it is nevertheless interesting to investigate the new physical effects that arise from the use of a molecular potential (with cylindrical symmetry) instead of the atomic one (with spherical symmetry). In particular, one can expect to uncover the general trends that govern the two-electron escape by two-photon absorption in a molecular system. The simplest approach to the molecular problem consists in assuming the validity of the fixed-nuclei approximation, in which the positions of the two nuclei are fixed at their equilibrium internuclear distance $R_e = 1.4$ a.u.. This has been shown to be an excellent approximation in one-photon double ionization of H_2 ([26, 27]) because the two electrons are ejected almost instantaneously and, therefore, the nuclei do not have time to move during the ionization process. However, in the two-photon ionization case, some caution is necessary, since double electron escape can also occur through a sequential process in which one electron is first ejected after absorption of one photon and the second electron is later ejected after absorption of the other photon. If the time delay between the first and the second electron ejection is long enough to allow the nuclei to move (which

is perfectly possible when, e.g., autoionizing states are active in the process -see e.g. [28, 29, 30]), any realistic description of the double ionization process must account for this nuclear motion. Fortunately, the sequential process is only possible for photon energies larger than 31 eV (this is the energy difference between the H_2^+ ground state and the H_2 double ionization continuum in the Franck-Condon region). Therefore, the fixed-nuclei approximation will be meaningful to study two-photon double ionization from the threshold up to 30 eV.

In a very recent communication, Colgan et al [1] have reported the first theoretical predictions of fully differential cross sections for two-photon double ionization of H_2 at 30 eV by solving the time-dependent Schrödinger equation. In this paper, we present the first accurate, time-independent calculations of this process using the exterior complex scaling method which has produced benchmark results for one- and two-photon double ionization of He [12, 15, 23] and one-photon double ionization of H_2 [15, 27, 26, 31]. This method provides grid-based, numerical solutions of the Schrödinger equation with no appeal to approximate asymptotic forms nor to ansatz wave functions. In order to compare with the predictions of reference [1], we have considered the same photon energy, 30 eV, and molecular orientations parallel and perpendicular to the polarization vector. We will see that, although these methods have led to almost perfect agreement for the one-photon double ionization of H_2 [32], they disagree in the two-photon case. In particular, we find that, when the molecule is ionized parallel to the polarization vector, the electrons are almost exclusively ejected back to back. This is similar to previous findings in Helium but it is somewhat in contradiction with the triply differential cross sections reported in [1]. A similar behavior is observed when the molecule is perpendicular to the polarization vector, which is in better agreement with the predictions of [1].

Atomic units are used throughout unless otherwise stated.

2. Methods

2.1. Exterior complex scaling treatment of molecular two-photon double ionization

The cross section for two-photon double ionization using lowest order perturbation theory (LOPT) in the velocity gauge, for a given internuclear distance, and differential in the electron energy sharing, and in the angular dependence of the ejected electrons is given by the expression:

$$\frac{d\sigma}{dE_1 d\Omega_1 d\Omega_2} = \frac{2\pi}{\hbar}\frac{(2\pi\alpha)^2}{m^2\omega^2} k_1 k_2 |f(\mathbf{k_1}, \mathbf{k_2}, \omega)|^2 \tag{1}$$

where $f(\mathbf{k_1}, \mathbf{k_2}, \omega)$ is the two-photon double ionization amplitude, $\mathbf{k_1}$ and $\mathbf{k_2}$ are the momenta of the photoelectrons, ω is the photon frequency, m is the electron mass and α is the fine-structure constant. The problem of obtaining the molecular double photo-ionization amplitude for the one-photon absorption case was correctly addressed in Ref.[26]. A straightforward generalization to the two-photon case allows us to write

the corresponding amplitude as the following integral for a given internuclear distance:

$$f(\mathbf{k_1},\mathbf{k_2}) = \langle \Phi^{(-)}(\mathbf{k_1},\mathbf{r_1})\Phi^{(-)}(\mathbf{k_2},\mathbf{r_2})|[E - T - v(\mathbf{r_1}) - v(\mathbf{r_2})]|\Psi_2^{SC}(\mathbf{r_1},\mathbf{r_2})\rangle \quad (2)$$

where E is the excess energy above the double ionization threshold, T is the two-electron kinetic energy operator and $v(\mathbf{r})$ is the nuclear attraction potential seen by one electron in the field of the bare nuclei. The functions $\Phi^{(-)}(\mathbf{k},\mathbf{r})$ are H_2^+ continuum eigenfunctions with incoming momentum $\mathbf{k}$. The use of those eigenfunctions as testing functions to extract the amplitudes is extensively explained in both [26] and [33]. This choice of testing functions is optimal for our purposes because the orthogonality of the H_2^+ continuum eigenfunctions to the bound states of H_2^+ eliminates the contributions of the single ionization channels to Equation (2). We must emphasize that the product of testing functions is not the physical final-state, which is included in $\Psi_2^{SC}(\mathbf{r_1},\mathbf{r_2})$. The latter wave function is the purely outgoing two-photon wave function, that is the solution of the coupled driven Schrödinger equations, in the Dalgarno-Lewis form of second-order perturbation theory that describe the absorption of two photons by a system initially in a state Φ_0:

$$(E_0 + \hbar\omega - H)|\Psi_1^{SC}(\mathbf{r_1},\mathbf{r_2})\rangle = \epsilon\cdot(\nabla_\mathbf{1} + \nabla_\mathbf{2})|\Phi_0\rangle \quad (3)$$

$$(E_0 + 2\hbar\omega - H)|\Psi_2^{SC}(\mathbf{r_1},\mathbf{r_2})\rangle = \epsilon\cdot(\nabla_\mathbf{1} + \nabla_\mathbf{2})|\Psi_1^{SC}\rangle \quad (4)$$

where ϵ is the polarization unit vector, ∇_1 and ∇_2 are the gradient operators for the electronic coordinates, and $|\Phi_0\rangle$ is the initial bound state of H_2. Notice that we have used the velocity form of the dipole operator. These two driven equations must be solved with the proper outgoing wave scattering boundary conditions. These conditions are imposed rigorously, as described in previous publications on this method [34], by transforming the radial coordinates of both electrons according to the exterior complex scaling (ECS) transformation. This transformation scales those coordinates by a complex factor, $\exp(i\eta)$ beyond some radius R_0:

$$r \rightarrow \begin{cases} r & \text{for} \quad r \leq R_0 \\ R_0 + (r - R_0)e^{i\eta} & \text{for} \quad r > R_0 \end{cases} \quad (5)$$

For photon energies below the first ionization potential of H_2, applying the ECS transformation to the electronic radial coordinates in Eq. (3) and (4) causes the purely outgoing solutions $\Psi_1^{SC}(\mathbf{r_1},\mathbf{r_2})$ and $\Psi_2^{SC}(\mathbf{r_1},\mathbf{r_2})$ to decay exponentially for any $r_i > R_0$, regardless of the number of electrons in the continuum. Thus choosing R_0 large enough, this method allows $\Psi_1^{SC}(\mathbf{r_1},\mathbf{r_2})$ and $\Psi_2^{SC}(\mathbf{r_1},\mathbf{r_2})$ to reach its correct outgoing asymptotic form where the $\mathbf{r_1}$ and $\mathbf{r_2}$ coordinates are real valued. In other words, the ECS transformation provides us with the physical wave function in the region where both coordinates are less than R_0. In an exact or converged calculation the solutions of the Schrödinger equation for $r < R_0$ do not depend on η or R_0.

In the present application of the ECS transformation we must also address a difficulty specific to the application of the ECS approach to two-photon double ionization, which, as pointed out in earlier studies on He [12, 23, 15], does not appear in the case of one-photon double ionization. For photon energies above the first ionization

potential of H_2, the solution of Equation (3), $\Psi_1^{SC}(\mathbf{r_1}, \mathbf{r_2})$, will have single-ionization terms that behave, at large *real* values of the electron coordinates, as the product of a bound state of H_2^+ times an undamped outgoing wave in the other electron coordinate. This means that $\epsilon \cdot (\nabla_\mathbf{1} + \nabla_\mathbf{2})|\Psi_1^{SC}$, which is the initial term for Equation (4), will not vanish as $\mathbf{r_1}$ or $\mathbf{r_2} \to \infty$ along the real axis. Because the dipole operator is a one-body operator, the application of outgoing boundary conditions via the ECS transformation in Equation (4) will depend on the value of R_0, irrespective of the gauge being used, and the amplitudes extracted from $\Psi_2^{SC}(r_1, r_2)$ will not converge with increasing volume of the space on which it is solved. To avoid this problem we can add a small, positive, imaginary part to ω in Eq. Equation (3) only. This will produce a solution $\Psi_1^{SC}(\mathbf{r_1}, \mathbf{r_2})$ with an exponential falloff for the real r values. In this way, $\Psi_1^{SC}(\mathbf{r_1}, \mathbf{r_2})$ will be a valid driving term for Equation (4). However, this procedure yields different amplitudes for different complex values of ω in the first equation. Thus Equation (3) and Equation (4) must be repeatedly solved for different values of the imaginary part of ω and then numerically extrapolated to a purely real photon energy.

As indicated above, all calculations have been carried out at the equilibrium internuclear distance $R_e = 1.4$ a.u., unless otherwise stated.

2.2. Numerical implementation

In these calculations we use numerical procedures similar to those used for one-photon double ionization of H_2 ([26, 27, 33]), in which we decompose the full scattered wave into angular components on a radial grid in order to implement exterior complex scaling. We expand the scattered wave functions that solve Equation (3) and Equation (4), for a fixed value of the projection M of the electronic angular momentum along the molecular axis and for singlet spin coupling, as a sum of products of two-dimensional radial wave functions and spherical harmonics:

$$\Psi^{SC,(M)} = \sum_{\mu_1\mu_2, j_1 \geq j_2} \left(\frac{\psi^{dir}_{j_1,\mu_1,j_2,\mu_2}(r_1, r_2)}{r_1 r_2} Y_{j_1\mu_1}(\hat{\mathbf{r}}_\mathbf{1}) Y_{j_2\mu_2}(\hat{\mathbf{r}}_\mathbf{2}) + \frac{\psi^{exch}_{j_1,\mu_1,j_2,\mu_2}(r_1, r_2)}{r_1 r_2} Y_{j_2\mu_2}(\hat{\mathbf{r}}_\mathbf{1}) Y_{j_1\mu_1}(\hat{\mathbf{r}}_\mathbf{2}) \right) \tag{6}$$

The radial functions $\psi^{dir}_{j_1,\mu_1,j_2,\mu_2}$ and $\psi^{exch}_{j_1,\mu_1,j_2,\mu_2}$ are expanded in products of discrete variable representation (DVR) basis functions, so that the Hamiltonian matrix elements corresponding to the left hand sides of Equation (3) and Equation (4) are the same as those in a "complete configuration interaction" calculation in that basis.

In this work, we will consider two possible orientations of the molecule with respect to the polarization vector: parallel and perpendicular. In the first case, $\Delta M = 0$ and the two photon transition is given by the following sequence of molecular symmetries (notice that ${}^1\Sigma_g^+$ is the symmetry of the ground state of H_2):

$${}^1\Sigma_g^+ \to^1 \Sigma_u^+ \to^1 \Sigma_g^+ \tag{7}$$

The corresponding amplitude can be written as:

$$f^{||}(\mathbf{k_1}, \mathbf{k_2}, \omega) = f_{^1\Sigma_g^+ \to {}^1\Sigma_u^+ \to {}^1\Sigma_g^+} \tag{8}$$

In the perpendicular case, $\Delta M = \pm 1$ and the possible transitions are:

$$\begin{aligned} &{}^1\Sigma_g^+ \to \Pi_u \to \Delta_g \\ &{}^1\Sigma_g^+ \to \Pi_u \to \Sigma_g^+ \end{aligned} \tag{9}$$

The corresponding amplitude is the coherent superposition of these two paths:

$$f^{\perp}(\mathbf{k_1}, \mathbf{k_2}, \omega) = f_{^1\Sigma_g^+ \to \Pi_u \to \Delta_g} + f_{^1\Sigma_g^+ \to \Pi_u \to \Sigma_g^+}. \tag{10}$$

When the molecular axis is not aligned either perpendicular or parallel to the polarization vector, we have a more complicated combination of amplitudes. The analysis of these orientations will be postponed to future work.

2.3. Test for two-photon single ionization

To check that our implementation of the ECS method for the two-photon molecular problem is correct, we have first evaluated the two-photon single ionization cross section of H_2 oriented parallel to the polarization vector. For this particular orientation there are previous results with which to compare [35, 36]. In this problem, the photon energy is smaller than the H_2 ionization potential and, consequently, there is no need to use a complex photon energy to solve the first driven equation (the second photon absorption connects a truly exponentially decreasing state with the final state). Figure 1 shows a comparison between our results and those previously reported in [35, 36]. The agreement is very good, especially with the more recent results of Palacios [36]. The observed peaks are associated with resonance enhanced multiphoton ionization (REMPI) that involves the $^1\Sigma_u^+$ bound states of H_2. It is important to emphasize here that these peaks are significantly broadened and enhanced when the vibrational motion is included [37]. This is due to the fact that, in REMPI, the nuclei have enough time to move during the ionization process and, consequently, Chase's approximation is no longer valid. In any case, this does not invalidate the comparison shown in Figure 1 since the only purpose is to show that the present implementation of the ECS method is correct.

2.4. Test of the Im[ω] $\to$ 0 extrapolation

As mentioned above, in two-photon double ionization of H_2, $\Psi_1^{SC,(M)}$ must be evaluated for different values of the imaginary part of ω, Im[ω]. This leads to transition amplitudes that depend on Im[ω] and, therefore, must be extrapolated to Im[ω] = 0. We have thoroughly tested different extrapolation methods, including linear, exponential, and polynomial extrapolations, in order to find which one leads to the best fit of the amplitudes and to the most stable extrapolated value. The chosen method is a fourth-order polynomial extrapolation method that includes all calculated amplitudes down to Im[ω] = 0.05. We have not included amplitudes for smaller values of Im[ω] because close to the limit Im[ω] = 0 they deviate rapidly from their smooth behavior in

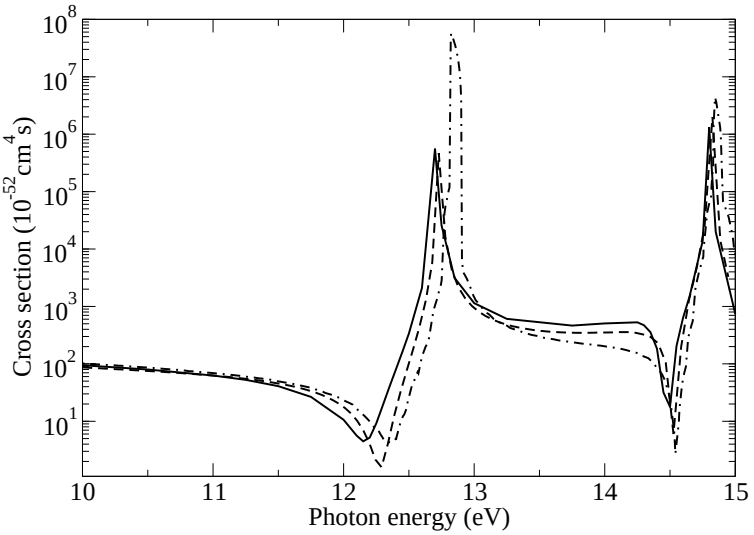

Figure 1. Two-photon single ionization cross sections of H_2 oriented parallel to the polarization vector. Full curve: present results obtained with a DVR basis with grid points placed at $\{0, 5, 15, 25, 35, 45, 55, 70\}$ a.u. and angular momentum up to 7 (176 angular configurations). Dashed line: Palacios [36]. Dashed-dotted line: Apalategui et al [35].

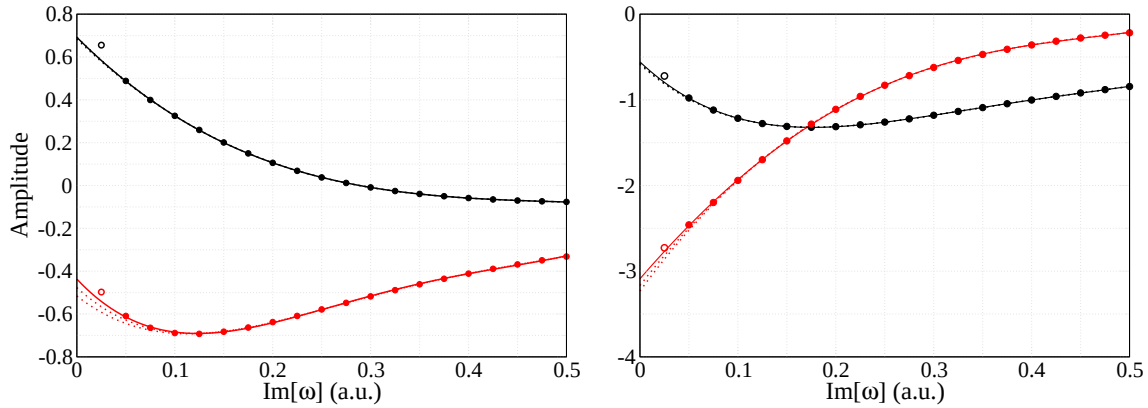

Figure 2. Examples of the extrapolation of the amplitudes to $\mathrm{Im}[\omega] = 0$ in atomic units. Solid line: fourth order polynomial fit of the amplitudes, including all points up to $\mathrm{Im}[\omega] = 0.05$, for a photon of 30 eV. Dashed lines, same as solid line, but including points up to $\mathrm{Im}[\omega] = 0.025$, 0.075, and 0.1. Left panel:$(l_1, l_2, j_1, m_1, j_2, m_2)$=$(1, 1, 1, 0, 1, 0)$ Σ_g^+ amplitude; left panel: $(1, 1, 1, -1, 1, -1)$ Δ_g amplitude.

the rest of the complex plane from which we are extrapolating. Figure 2 illustrates the performance of the fourth-order polynomial extrapolation for two characteristic amplitudes: the dominant ones leading to $^1\Sigma_g^+$ and $^1\Delta_g$ final symmetries. It can be seen that the extrapolation value is very stable with respect to the smallest value of $\mathrm{Im}[\omega]$ included in the fit. We have found a similar stability for other amplitudes and for the calculated cross sections (see Figure 3). Hence, in practice, the extrapolation

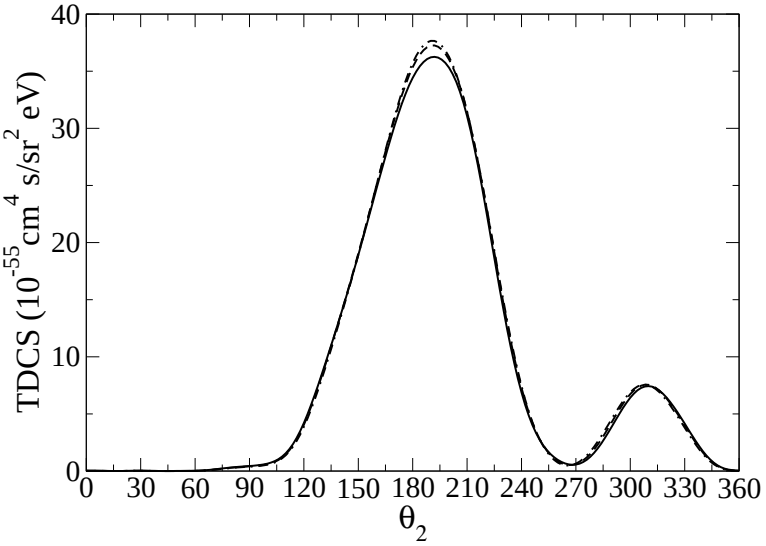

Figure 3. TDCS for a photon energy of 30 eV, the molecule oriented perpendicular to the polarization vector, and an angle for the fixed electron of 30 degrees. Grid points set at $\{0, 5, 10, 20, 30, 40, 50, 60, 70, 80, 90, 100, 110, 120, 130, 140, 150, 170\}$ atomic units. Angular momentum up to 7 (161 angular configurations for Δ_g states, and 176 for the Σ_g^+ states). Solid line: including all points up to Im$[\omega] = 0.05$. Dashed line: including all points up to Im$[\omega]$ 0.075. Dashed-dotted line: including all points up to Im$[\omega]$ up to 0.1.

is performed automatically by imposing that all amplitudes calculated in the interval $0.05 \leq \text{Im}[\omega] \leq 0.5$ are included in the fit to the fourth-order polynomial.

2.4.1. Basis set convergence We have performed calculations with different box sizes, different DVR grids and different values of angular momentum. As we can see in Figure 4, at a photon energy of 30 eV, convergence is reached for $l_{max} = 8$, a box size of 170 a.u. ($R_0 = 140$ a.u.), and a DVR grid 0, 5, 10, 20, 30, 40, 50, 60, 70, 80, 90, 100, 110, 120, 130, 140, 150, 170 a.u.. Results obtained with $l_{max} = 7$ and/or slightly smaller boxes and/or slightly less dense DVR grids are very similar. We have checked that results obtained with different angles of the complex rotation are indistinguishable in the scale of the figure. All results reported below have been obtained by using the largest basis set.

2.4.2. United atom limit We have performed calculations for two-photon double ionization of H_2 by using a value of the internuclear distance of 0.1 a.u.. In this case, the fully differential cross sections for parallel and perpendicular orientations must be almost identical and very similar to the corresponding Helium ones for the same excess photon energy. Figure 5 shows the calculated cross sections for an excess photon energy of 42 eV for the parallel and perpendicular cases. As can be seen, for all ejection directions of the fixed electron, the results for both orientations are indeed very close to each other. The success of this test proves that coherence between the different amplitudes

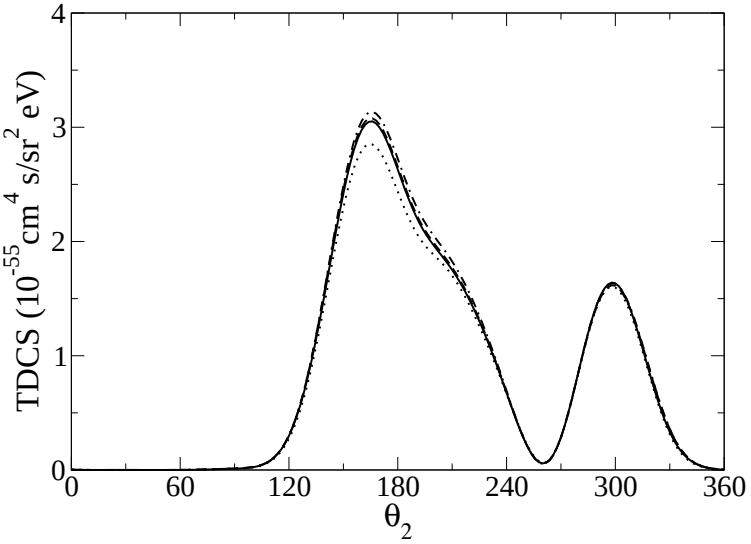

Figure 4. TDCS for a photon of 30 eV, Im[ω] = 0.05, and a fixed electron angle of 30 degrees, for H_2 parallel to the polarization vector. Solid: DVR grid in a.u. $\{0, 5, 10, 20, 30, 40, 50, 60, 70, 80, 90, 100, 110, 120, 130, 140, 150, 170\}$, $R_0 = 140 a.u.$, $l_{max} = 8$. Dashed: Same grid as before but with $l_{max} = 7$. Dotted: DVR grid in a.u. $\{0, 5, 10, 20, 30, 40, 50, 60, 70, 80, 90, 100, 110, 120, 130\}$, $R_0 = 110 a.u.$, $l_{max} = 7$. Dash-dotted: DVR grid in a.u. $\{0, 5, 10, 20, 31.25, 42.5, 54.75, 66, 77.25, 88.5, 99.75, 110, 120, 130\}$, $R_0 = 110 a.u.$, $l_{max} = 7$.

calculated with our H_2 code is correctly described. The figure also includes the He results previously reported in references [7, 15, 19, 38] for the same excess photon energy and the same angles of the fixed electron. The cross sections calculated with $R = 0.1$ a.u. agree qualitatively with the Helium ones reported in references [15, 19, 38] at $\theta_1 = 0$ and 30°; the agreement deteriorates at $\theta_1 = 60$ and 90° because the corresponding cross sections are substantially smaller. The cross sections reported in [7] are systematically lower than those reported in [15, 19, 38]. In assessing the quality of the present results one must take into account the fact that we are not using exactly $R = 0$ in the molecular calculations (the reason for not doing it is that it would be a source of numerical errors in our molecular code) and that the differences among the three Helium calculations that better agree in magnitude are of the order of those between the latter and the present calculations. Extrapolating the conclusions of this analysis to the true molecular case ($R = 1.4$ a.u.) suggests that the error of the cross sections presented in the following sections should not be larger than 30%.

3. Results and discussion

The calculated triply differential cross sections for two-photon double ionization are given in Figs. 6 and 7 for molecules oriented, respectively, parallel and perpendicular to the polarization vector. All the results correspond to equal energy sharing between

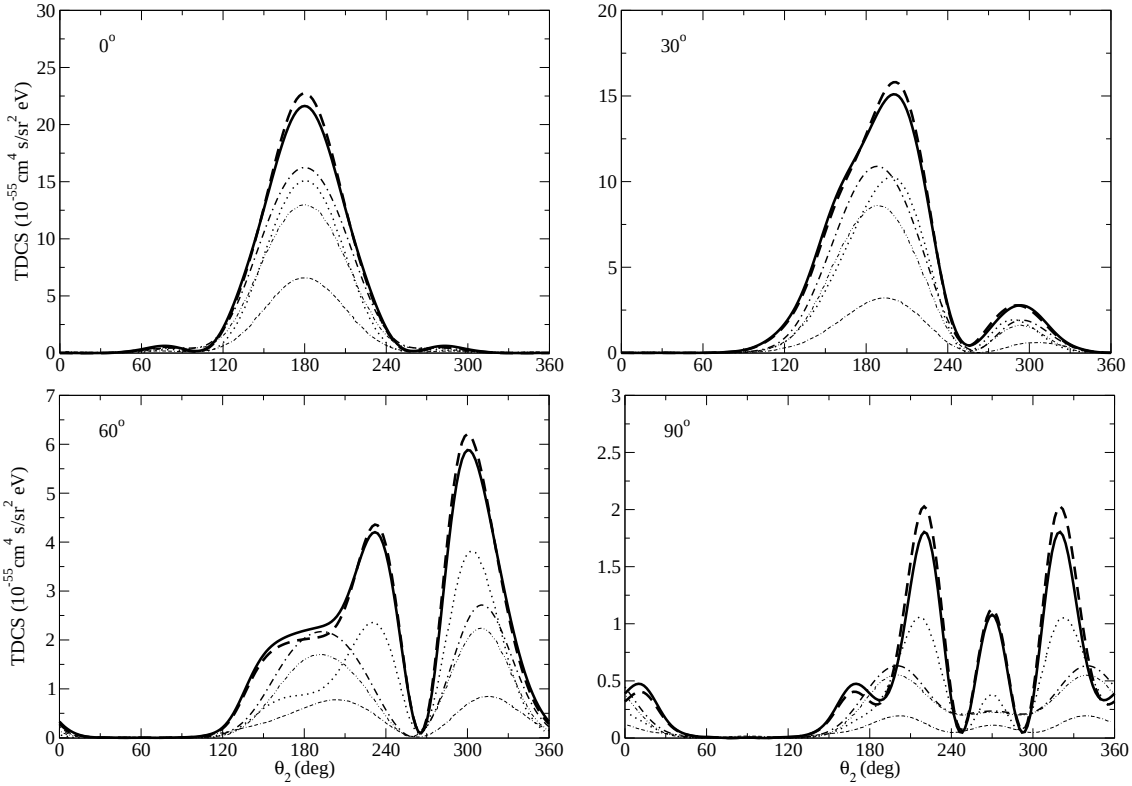

Figure 5. TDCS of He and H_2 oriented parallel and perpendicular to the polarization direction for an excess photon energy of 42 eV, equal energy sharing and emission angles of the fixed electron 0, 30, 60 and 90°. The TDCS is shown in the plane that contains the direction of the fixed electron and the polarization vector. The H_2 internuclear distance is $R = 0.1$. Amplitudes where extrapolated using the same procedure as described above. The basis details are the same as those given in figure (3). Thick solid line: H_2 parallel. Thick dashed line: H_2 perpendicular. Dotted line: He results from [15]. Dashed-dotted lines: He results from [38]. Dashed-double dotted lines: He results from [19]. Dotted-double dashed lines: He results from [7].

the electrons. The TDCS are plotted in the plane formed by the molecular axis, the polarization vector and the direction of ejection of the fixed electron. In the top left panel of Figure 6, the molecular axis, the polarization direction and the direction of the fixed electron coincide at 0°. In the three remaining panels of Fig. 6, the direction of the fixed electron is rotated $\theta_1 = 30$, 60 and 90°, respectively, with respect to the the polarization vector (and the molecular axis). In the top left panel of Figure 7, the polarization vector and the direction of the fixed electron coincide, and the molecular axis is perpendicular to them. In the other three panels, the direction of the fixed electron is rotated by $\theta_1 = 30$, 60 and 90° with respect to the the polarization vector. Notice that, in both figures, the TCDS is largest for $\theta_1 = 0°$ and then decreases with θ_1. The TDCS for $\theta_1 = 90°$ is roughly an order of magnitude smaller than that for $\theta_1 = 0°$ in the parallel case (figure 6) and two orders of magnitude smaller than that for $\theta_1 = 0°$ in the perpendicular case (figure 7). For $\theta_1 = 0°$, the second electron preferentially escapes

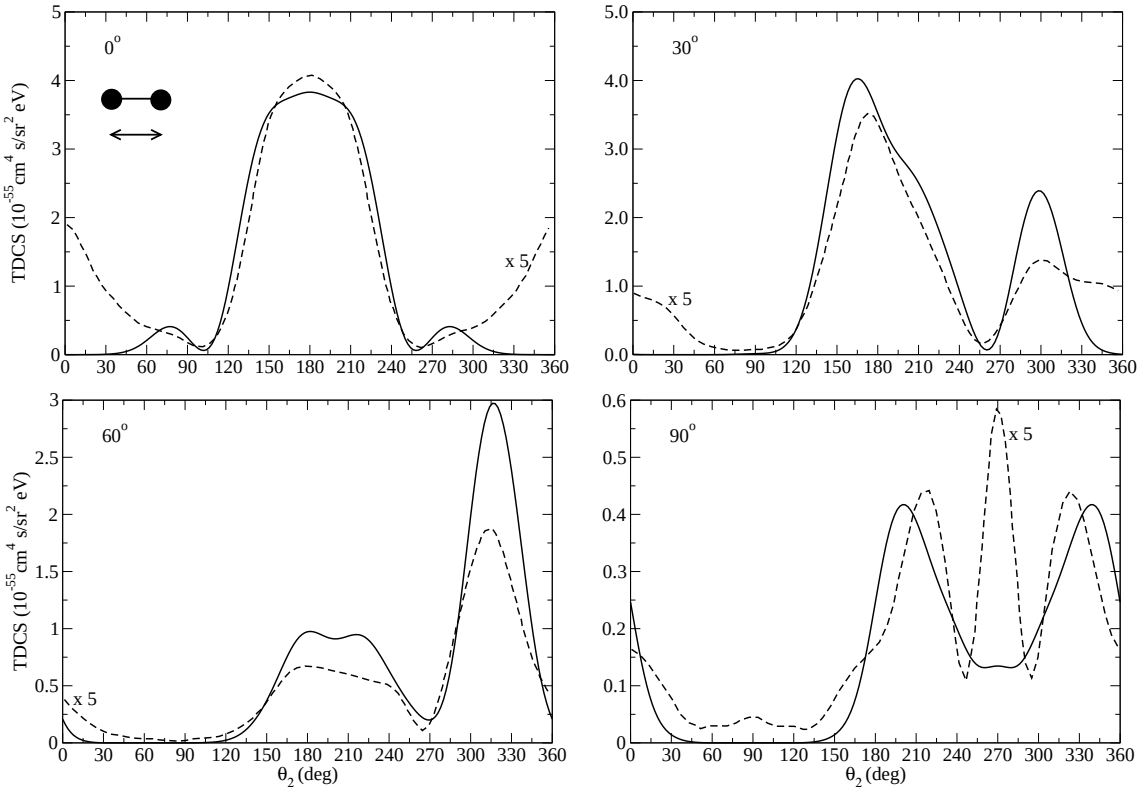

Figure 6. TDCS for a photon energy of 30 eV with the molecule oriented parallel to the polarization axis. Each panel displays a different orientation of the fixed electron. Solid: ECS calculations using a DVR grid in a.u. $\{0, 5, 10, 20, 30, 40, 50, 60, 70, 80, 90, 100, 110, 120, 130, 140, 150, 170\}$, $R_0 = 140 a.u.$, $l_{max} = 8$. Dashed: Results from [1] multiplied by 5.

at 180°, i.e., in a direction opposite to that of the first electron. This is similar to what has been found in two-photon double ionization of Helium [14, 15, 16]. In contrast, as θ_1 increases, there is less and less tendency of the electrons to escape in opposite directions. Also, the difference between the parallel and the perpendicular orientations become more apparent. Both effects are the consequence of molecular effects not present in Helium.

The present results are compared with those previously obtained by Colgan et al [1]. In the parallel case, our calculated TDCSs are approximately a factor of five larger than those reported in [1]. In the perpendicular case, the magnitudes are more similar. There are also important differences in the shapes of the TDCSs. For all the TDCSs plotted in Figs. 6 and 7, there is an effective node in the cross section when $\theta_1 = \theta_2$, i.e., we predict zero probability for the second electron to escape in the same direction as the first electron. (Bear in mind that we are reporting TDCS for equal energy sharing.) This is not the case in the TDCS reported by Colgan et al [1], especially for the parallel orientation at $\theta_1 = \theta_2 = 0°$, where they predict that the probability for both electrons to escape in the same direction is about 50% of the probability to escape in opposite

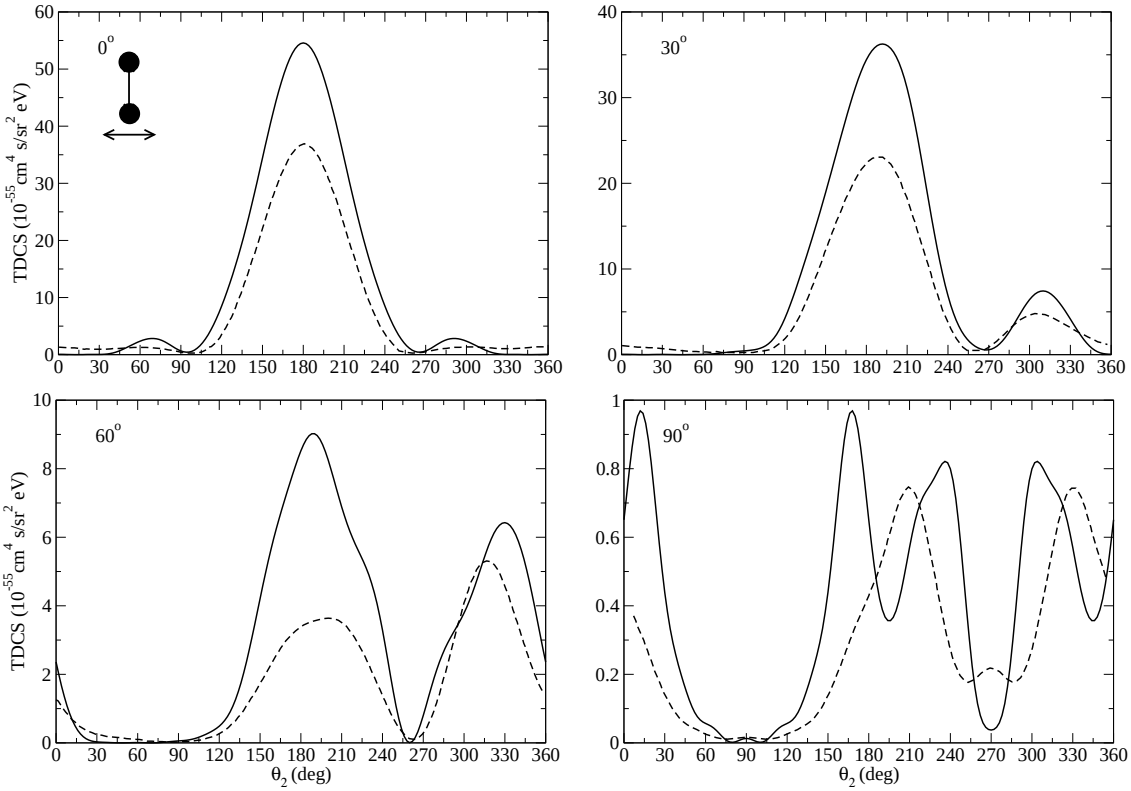

Figure 7. TDCS for a photon energy of 30 eV with the molecule oriented perpendicular to the polarization axis. Each panel displays a different orientation of the fixed electron. Solid: ECS calculations using a DVR grid in a.u. $\{0, 5, 10, 20, 30, 40, 50, 60, 70, 80, 90, 100, 110, 120, 130, 140, 150, 170\}$, $R_0 = 140 a.u.$, $l_{max} = 8$. Dashed: Results from [1]

directions. This result is striking because, in Helium, all existing calculations report an effective node that prevents both electrons from escaping in the same direction when they have the same energy (see figure 5 and references [7, 15, 19, 38]). Physical intuition suggests that this should be also the case in two-photon double ionization of H_2 because Coulomb repulsion demands this to be so. In general, the TDCSs reported by Colgan et al are more helium-like than ours: theirs are more similar to the Helium TDCSs and they do not differ significantly in the parallel and perpendicular orientations. For instance, for $\theta_1 = 60°$, they find the same relative magnitude of the two main peaks in the parallel and the perpendicular orientations, while we find opposite relative magnitudes in each orientation. While it is very difficult to know the reason why molecular effects are stronger in the present results, all consistency tests reported in the previous section suggest that this cannot be due to a lack of convergence.

Acknowledgments

Work performed under the auspices of the Spanish Ministerio de Ciencia e Innovación (contract No. FIS2007-60064), the European Science Foundation (COST action

CM0702), the US DOE by Los Alamos National Laboratory (contract No. DE-AC52-06NA25396) and Lawrence Berkeley National Laboratory (contract No. DE-AC02-05CH11231), and supported by the US DOE Office of Basic Energy Sciences, Division of Chemical Sciences. CWM acknowledge support from the National Science Foundation (Grant No. PHY-0604628). All calculations were performed at the Barcelona Supercomputer Center Mare Nostrum (Spain).

References

[1] Colgan J, Pindzola M S, and Robicheaux F. Two-photon double ionization of the hydrogen molecule. *J. Phys. B: At. Mol. Opt. Phys.* , 41(12):121002, 2008.

[2] Proulx D, Pont M, and Shakeshaft R. Multiphoton detachment, ionization, and simultaneous excitation of two-electron systems. *Phys. Rev. A*, 49(2):1208–1213, Feb 1994.

[3] Nikolopoulos L A A and Lambropoulos P. Multichannel theory of two-photon single and double ionization of helium. *J. Phys. B: At. Mol. Opt. Phys.* , 34(4):545, 2001.

[4] Colgan J and Pindzola M S. Core-excited resonance enhancement in the two-photon complete fragmentation of helium. *Phys. Rev. Lett.* , 88(17):173002, Apr 2002.

[5] Feng L and van der Hart H W. Two-photon double ionization of he. *J. Phys. B: At. Mol. Opt. Phys.* , 36(1):L1, 2003.

[6] Piraux B, Bauer J, Laulan S, and Bachau H. Probing electron-electron correlation with attosecond pulses. *The European Physical Journal D - Atomic, Molecular, Optical and Plasma Physics*, 26(1):7–13, 2003.

[7] Hu S X, Colgan J, and Collins L A. Triple-differential cross-sections for two-photon double ionization of he near threshold. *J. Phys. B: At. Mol. Opt. Phys.* , 38(1):L35, 2005.

[8] P. Lambropoulos, L. A. A. Nikolopoulos, and M. G. Makris. Signatures of direct double ionization under xuv radiation. *Phys. Rev. A*, 72(1):013410, Jul 2005.

[9] Foumouo E, Kamta G L, Edah G, and Piraux B. Theory of multiphoton single and double ionization of two-electron atomic systems driven by short-wavelength electric fields: An ab initio treatment. *Phys. Rev. A*, 74(6):063409, 2006.

[10] Kheifets A S and Ivanov I A. Convergent close-coupling calculations of two-photon double ionization of helium. *J. Phys. B: At. Mol. Opt. Phys.* , 39(7):1731, 2006.

[11] Shakeshaft R. Two-photon single and double ionization of helium. *Phys. Rev. A*, 76(6):063405, 2007.

[12] Horner D A, Morales F, Rescigno T N, Martín F, and McCurdy C W. Two-photon double ionization of helium above and below the threshold for sequential ionization. *Phys. Rev. A*, 76(3):030701, 2007.

[13] Nikolopoulos L A A and Lambropoulos P. Time-dependent theory of double ionization of helium under xuv radiation. *J. Phys. B: At. Mol. Opt. Phys.* , 40(7):1347, 2007.

[14] Ivanov I A and Kheifets A S. Two-photon double ionization of helium in the region of photon energies 42-50 ev. *Phys. Rev. A*, 75(3):033411, 2007.

[15] Horner D A, McCurdy C W, and Rescigno T N. Triple differential cross sections and nuclear recoil in two-photon double ionization of helium. *Phys. Rev. A*, 78(4):043416, 2008.

[16] Foumouo E, Antoine P, Piraux B, Malegat L, Bachau H, and Shakeshaft R. Evidence for highly correlated electron dynamics in two-photon double ionization of helium. *J. Phys. B: At. Mol. Opt. Phys.* , 41(5):051001, 2008.

[17] Foumouo E, Antoine P, Bachau H, and Piraux B. Attosecond timescale analysis of the dynamics of two-photon double ionization of helium. *New Journal of Physics*, 10(2):025017, 2008.

[18] Lambropoulos P, Nikolopoulos L A A, Makris M G, and Mihelič A. Direct versus sequential double ionization in atomic systems. *Phys. Rev. A*, 78(5):055402, 2008.

[19] Feist J, Nagele S, Pazourek R, Persson E, Schneider B I, Collins L A, and Burgdörfer J. Nonsequential two-photon double ionization of helium. *Phys. Rev. A*, 77(4):043420, 2008.

[20] Hasegawa H, Takahashi E J, Nabekawa Y, Ishikawa K L, and Midorikawa K. Multiphoton ionization of He by using intense high-order harmonics in the soft-x-ray region. *Phys. Rev. A*, 71(2):023407, Feb 2005.

[21] Sorokin A A, Wellhöfer M, Bobashev S V, Tiedtke K, and Richter M. X-ray-laser interaction with matter and the role of multiphoton ionization: Free-electron-laser studies on neon and helium. *Phys. Rev. A*, 75(5):051402, 2007.

[22] Rudenko A, Foucar L, Kurka M, Ergler Th, Kuhnel K U, Jiang Y H, Voitkiv A, Najjari B, Kheifets A, Ludemann S, Havermeier, T, Smolarski M, Schossler S, Cole K, Schoffler M, Dorner R, Dusterer S, Li W, Keitel B, Treusch R, Gensch M, Schroter C D, Moshammer R, and Ullrich J. Recoil-ion momentum distributions for two-photon double ionization of he and ne by 44 ev free-electron laser radiation. *Phys. Rev. Lett.*, 101:073003, 2008.

[23] Horner D A, Rescigno T N, and McCurdy C W. Decoding sequential versus nonsequential two-photon double ionization of helium using nuclear recoil. *Phys. Rev. A*, 77(3):030703, 2008.

[24] Antoine Ph, Foumouo E, and Piraux B. Two-photon double ionization of helium: an experimental lower bound of the total cross section. *Phys. Rev. A*, 78:023415, 2008.

[25] Jiang Y H, Moshammer R, Foucar L, Rudenko A, Kurka M, Schröter, Ergler Th, Kühnel K U, Lüdemann S, Schöffler M, Schössler S, Havermeier T, Smolarski M, Cole K, Dörner R, Düsterer S, Treusch R, Gensch M, and Ullrich J. Molecular fragmentation dynamics induced by sequential few photon absorption at flash. *Abstracts of the 11th International Conference on Multiphoton Processes*, page Mo03, 2008.

[26] Vanroose W, Horner D A, Martín F, Rescigno T N, and McCurdy C W. Double photoionization of aligned molecular hydrogen. *Phys. Rev. A*, 74(5):052702, 2006.

[27] Vanroose W, Martin F, Rescigno T N, and McCurdy C W. Complete Photo-Induced Breakup of the H_2 Molecule as a Probe of Molecular Electron Correlation. *Science*, 310(5755):1787–1789, 2005.

[28] I. Sánchez and F. Martín. *Phys. Rev. Lett.* , 79:1654–1657, 1997.

[29] F. Martín. *J. Phys. B: At. Mol. Opt. Phys.* , 32:R197–R231, 1999.

[30] Martín F, Fernández J, Havermeier T, Foucar L, Weber Th, Kreidi K, Schöffler M, Schmidt L, Jahnke T, Landers A L, Jagutzki O, Czasch A, Benis E, Osipov T, Belkacem A, Prior M H, Schmidt-Böcking H, Cocke C L, and Dörner R. Single photon-induced symmetry breaking H_2 dissociation. *Science*, 315:629, 2007.

[31] Horner D A, Miyabe S, Rescigno T N, McCurdy C W, Morales F, and Martín F. Classical two-slit interference effects in double photoionization of molecular hydrogen at high energies. *Phys. Rev. Lett.* , 101(18):183002, 2008.

[32] Colgan J, Pindzola M S, and Robicheaux F. Triple differential cross sections for the double photoionization of H_2. *Phys. Rev. Lett.*, 98:153001, 2007.

[33] Vanroose W, Martín F, Rescigno T N, and McCurdy C W. Nonperturbative theory of double photoionization of the hydrogen molecule. *Phys. Rev. A*, 70(5):050703, Nov 2004.

[34] McCurdy C W, Baertschy M, and Rescigno T N. *J. Phys. B*, 37:R137, 2004.

[35] Apalategui A and Saenz A. Multiphoton ionization of the hydrogen molecule H_2. *J. Phys. B: At. Mol. Opt. Phys.* , 35(8):1909, 2002.

[36] Palacios A. *Ionización y disociación de H_2^+ y H_2 por pulsos láser ultracortos en la región XUV.* PhD thesis, Universidad Autónoma de Madrid, 2006.

[37] Palacios A, Bachau H, and Martín F. Enhancement and control of H_2 dissociative ionization by femtosecond vuv laser pulses. *Phys. Rev. Lett.* , 96(14):143001, 2006.

[38] Palacios A, Rescigno T N, and McCurdy C W. Time-dependent treatment of two-photon resonant single and double ionization of helium by ultrashort laser pulses. *Phys. Rev. A*, submitted.